Supporting Information

Atomic-Scale Observation of Irradiation-Induced Surface Oxidation by In-Situ Transmission Electron Microscopy

Xing Huang, Travis Jones, Hua Fan, and Marc-Georg Willinger**

Dr. X. Huang, Dr. T. Jones, Dr. H. Fan, Dr. M. G. Willinger

Department of Inorganic Chemistry, Fritz-Haber Institute of Max-Planck Society, Faradayweg 4-6, 14195, Berlin, Germany.

Email: xinghuang0214@mail.ipc.ac.cn; xinghuang@fhi-berlin.mpg.de (X. Huang); willinger@fhi-berlin.mpg.de (M. G. Willinger)

Keywords: in-situ TEM, electron-beam irradiation, surface oxidation, sulfur vancancy, CdS

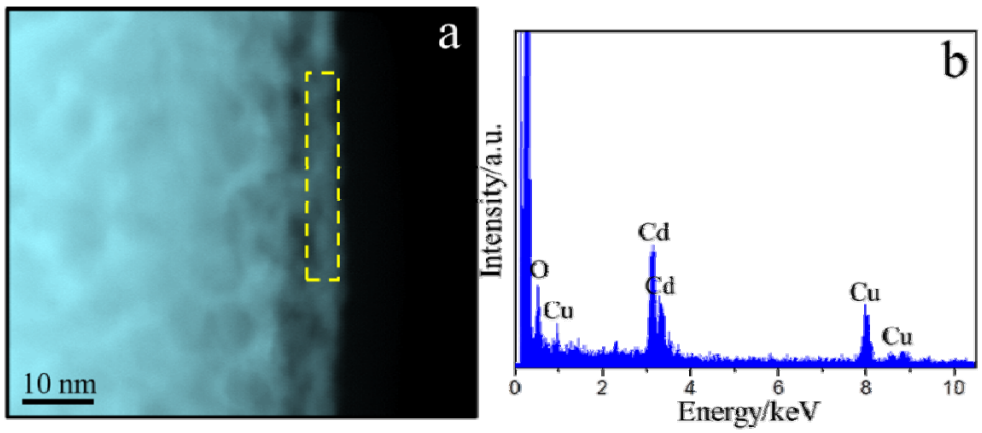

Figure S1. (a) HAADF-STEM image of the CdS ribbon after electron beam illumination; (b) EDX spectrum of the region labelled with the dished rectangle, showing the composition of CdO.

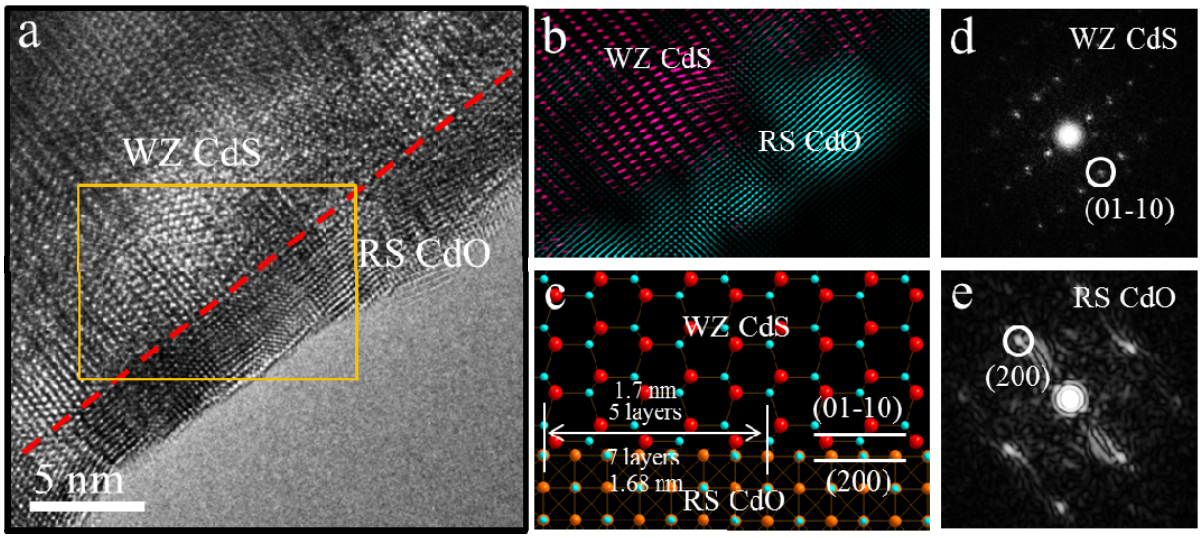

Figure S2. (a) HRTEM image of (01-10) surfaced CdS ribbon; (b) Reconstructed HRTEM image from the marked region shown in Figure S2a; (c) Corresponding atomic model; (d,e) FFT pattern from wurtzite (WZ) CdS and rock salt (RS) CdO domains. Red dashed line indicates the interface between the CdO and the CdS.

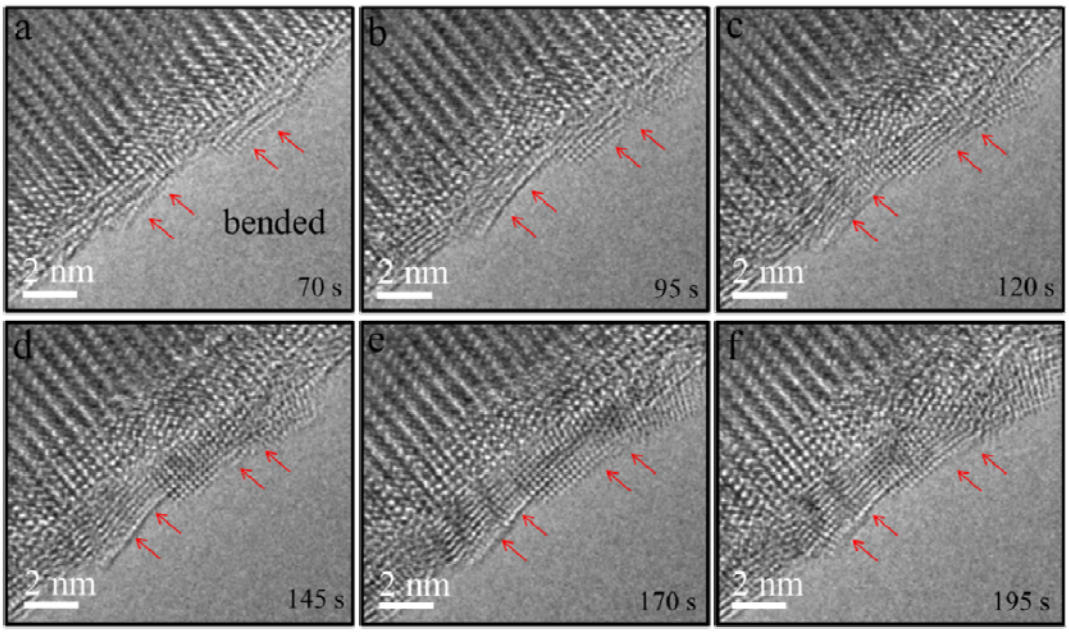

Figure S3. A series of HRTEM images showing the stress induced bending of growing CdO.

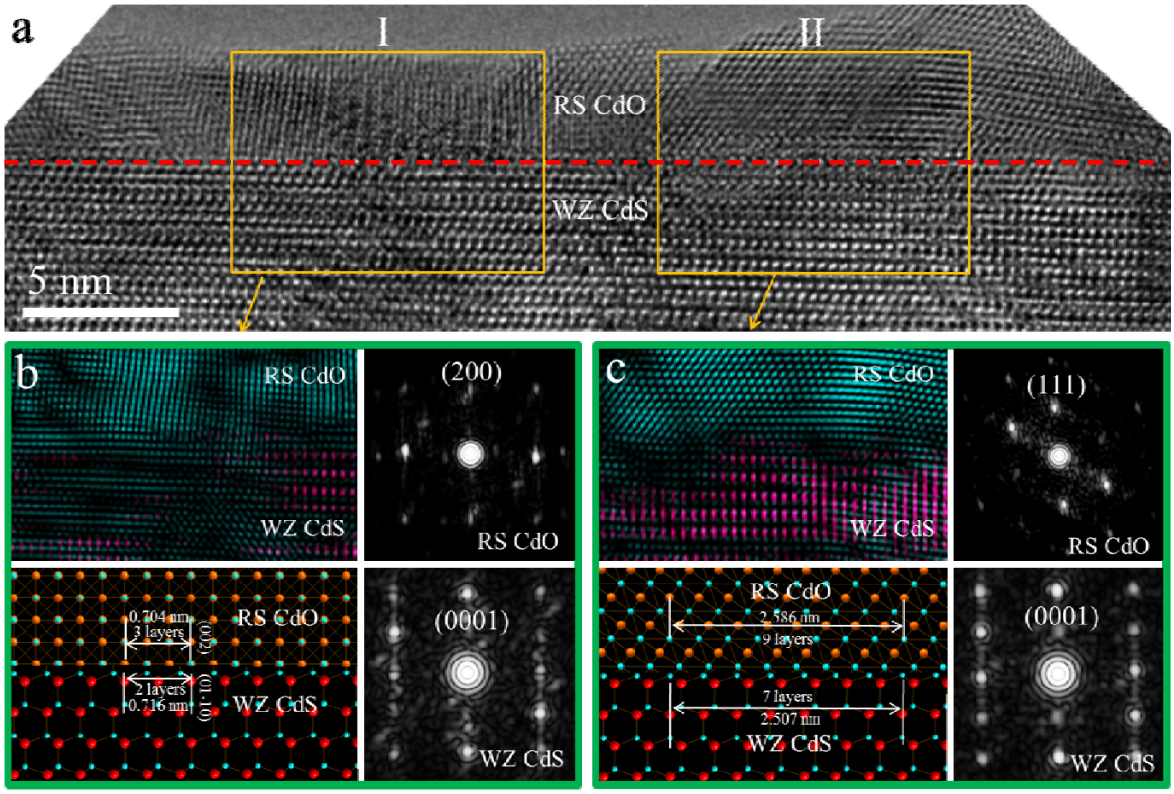

Figure S4. (a) HRTEM image of (0001) surfaced CdS ribbon; (b) Reconstructed HRTEM from region I and the corresponding atomic model, as well as the FFT pattern of CdS and CdO domains; (c) Reconstructed HRTEM from region II and the corresponding atomic model, as well as the FFT pattern of CdS and CdO domains. Red dashed line indicates the interface between the CdO and the CdS.

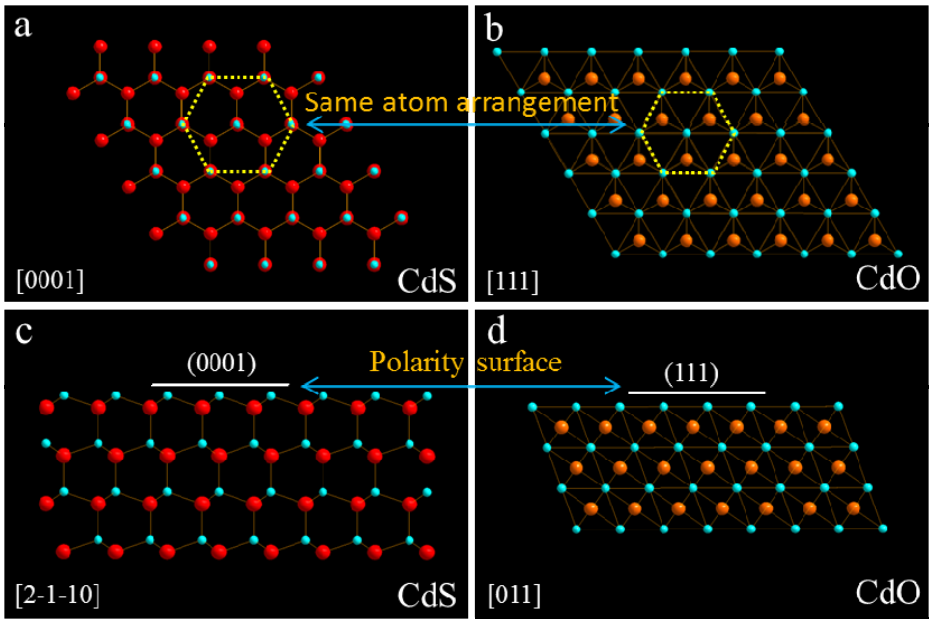

Figure S5. (a,c) Atomic models of WZ CdS viewed from [0001] and [2-1-10] zone axes; (b,d) Atomic models of RS CdO viewed from [111] and [011] zone axes.

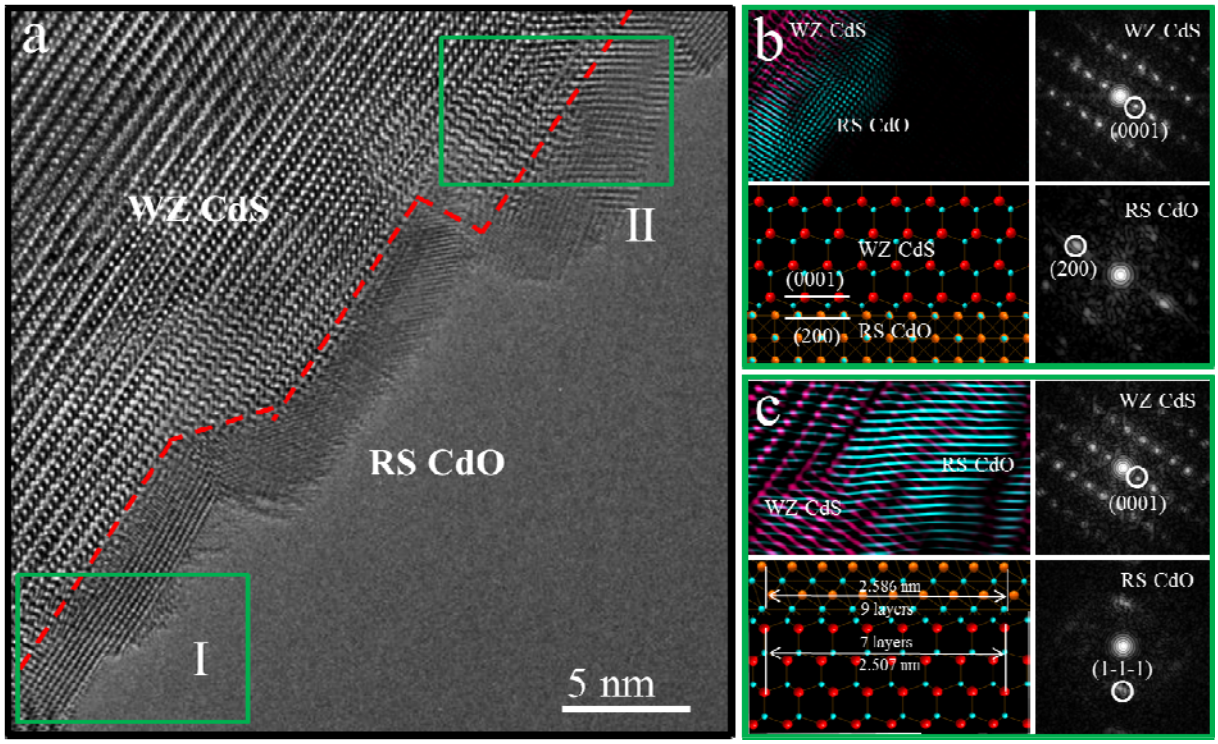

Figure S6. (a) HRTEM image of (0001) surfaced CdS ribbon; (b) Reconstructed HRTEM from region I and the corresponding atomic model, as well as the FFT pattern of CdS and CdO domains; (c) Reconstructed HRTEM from region II and the corresponding atomic model, as well as the FFT pattern of CdS and CdO domains. Red dashed line indicates the interface between the CdO and the CdS.

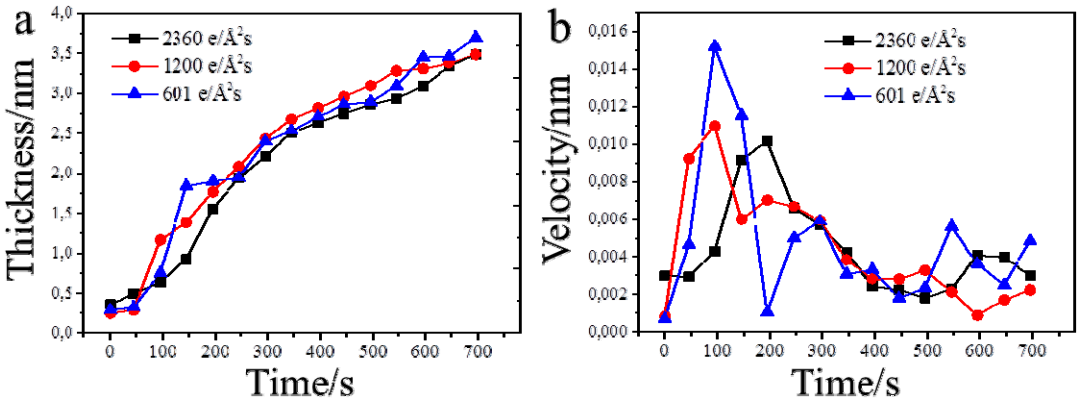

Figure S7. (a) Cumulative thickness of the CdO under different dose rates as a function of time; (b) Growth speed of CdO as a function of time derived from Figure S7a.

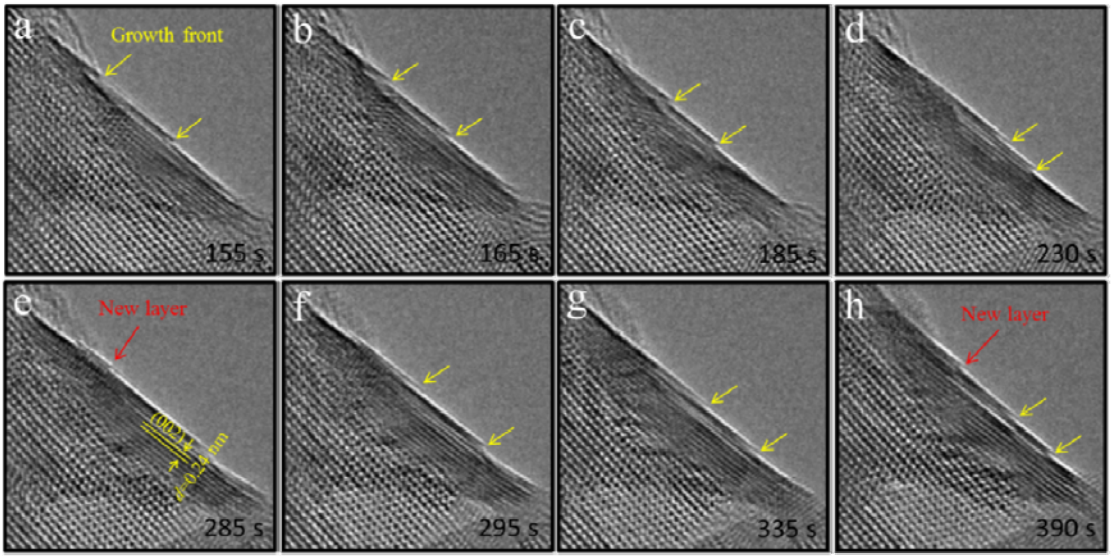

Figure S8. Series of HRTEM images showing a layer by layer growth of CdO from a broken spot of carbon layer.

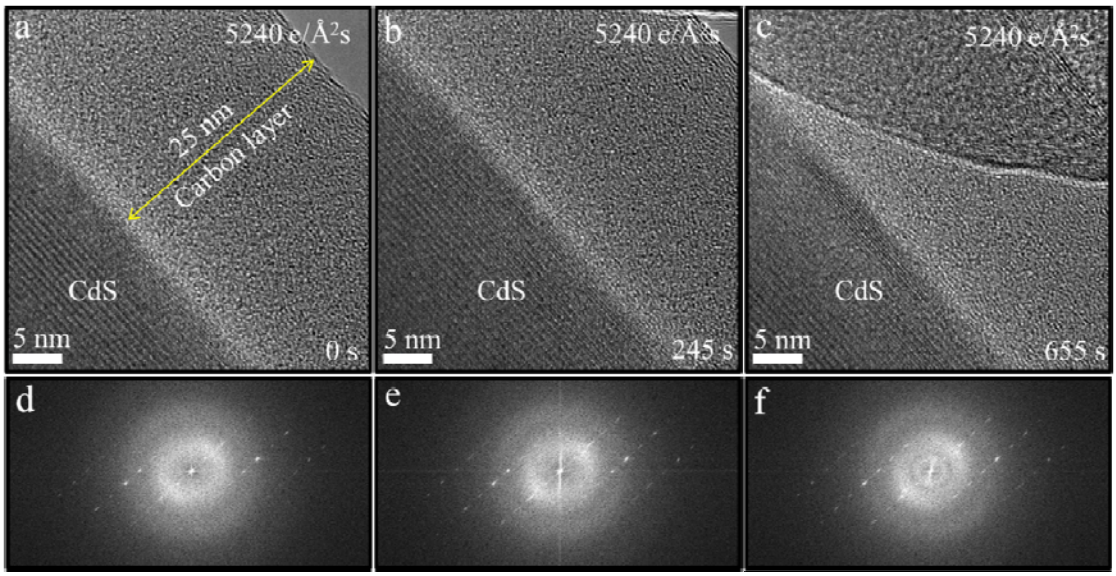

Figure S9. A series of (a-c) HRTEM images and (d-f) corresponding FFT patterns, showing that coverage of thick carbon layer is able to freeze the structure damage of CdS and its transition.

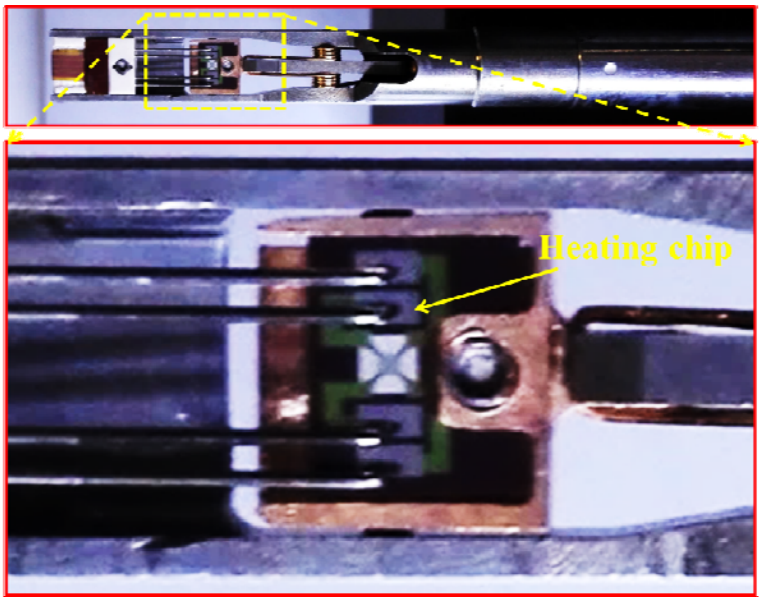

Figure S10. Optical image of the front a heating holder mounted with a heating chip as the sample carrier.

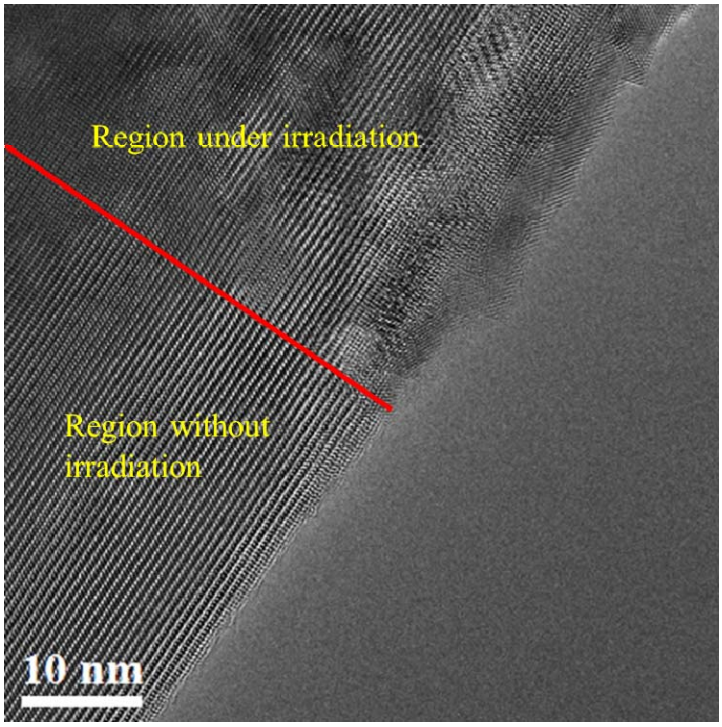

Figure S11. HRTEM image of a CdS ribbon that was partially irradiated by the electron beam. The region under the irradiation shows a clear structure transition on the surface whereas the region (without irradiation) right next to it barely shows changes. The red line indicates the bonduary between the regions with and without electron-beam irradiation.

Movie M1

In-situ TEM observation of CdS (01-10), (0001) and (03-31) planes under a constant dose rate of 5330e/Å^{2}s.

Movie M2

In-situ TEM observation of CdS (0001) plane under varied dose rates of 2360, 1200, 601 e/Å^{2}s.

Movie M3

In-situ TEM observation of CdS (0001) plane under electron dose rates of 311, 2380 and 5390 e/Å^{2}s.

Movie M4

In-situ TEM observation of carbon-coated CdS (0001) plane under a dose rate of 5240Å^{2}s, showing no structure transition or damage.

Movie M5

In-situ TEM observation of the CdS ribbon under a dose rate of 6480 e/Å^{2}s at 300°C and room temperature, respectively, revealing that the oxygen species contributed for the CdO formation is from the TEM column.